NANO EXPRESS

Nanofluids Containing γ-Fe₂O₃ Nanoparticles and Their Heat Transfer Enhancements

Shou-Zhu Guo · Yang Li · Ji-Sen Jiang · Hua-Qing Xie

Abstract Homogeneous and stable magnetic nanofluids containing γ-Fe₂O₃ nanoparticles were prepared using a two-step method, and their thermal transport properties were investigated. Thermal conductivities of the nanofluids were measured to be higher than that of base fluid, and the enhanced values increase with the volume fraction of the nanoparticles. Viscosity measurements showed that the nanofluids demonstrated Newtonian behavior and the viscosity of the nanofluids depended strongly on the tested temperatures and the nanoparticles loadings. Convective heat transfer coefficients tested in a laminar flow showed that the coefficients increased with the augment of Reynolds number and the volume fraction.

Keywords γ-Fe₂O₃ nanoparticle · Magnetic nanofluid · Thermal conductivity · Viscosity · Heat transfer coefficient

Introduction

Nanofluids, which contain nanoparticles dispersed in base fluids, have been proposed as a new kind of heat transfer media because they can improve the heat transport and energy efficiency and may have potential applications in the field of heat transfer enhancement. The thermal conductivity of the nanofluids can be enhanced obviously when nanoparticles, such as CNTs [1], Fe [2], Cu [3], and Al₂O₃ [4], are dispersed into the base fluids. Viscosity of the fluids also increases with the augment of the nanoparticles concentrations [5, 6] when nanoparticles are dispersed into the base fluids as well. At the same time, temperature and nanoparticles size [6] may have effects on the viscosity of the nanofluids. According to the previous studies [7–9], nanofluids can improve the convective heat transfer coefficient considerably comparing to the conventional heat transfer fluids and can be used in thermal devices or systems such as heat exchangers or cooling system to enhance heat transfer.

Magnetic fluids, suspension containing magnetic nanoparticles, show both magnetic and fluid properties and have important applications in industrial [10, 11] and biomaterial fields [12–14]. However, seldom experiments and applications on the heat transfer of magnetic fluids have been reported. The conductivity of magnetic nanofluids could be improved through controlling the alignment of nanoparticles by the external magnetic field [15]. What's more, with the development of the industry and the technology, the performance elevation of the traditional heat transfer medium using mixture of water and ethylene glycol (EG) is necessary. Kulkarni et al. [16] investigated the thermal properties of aluminum oxide nanofluids based on the mixture of EG and water. And they found that the heat transfer was enhanced efficiently.

In the present paper, γ-Fe₂O₃ nanoparticles were chosen to form nanofluids with mixture base fluid composed of 55 vol% deionized water (DW) and 45 vol% EG. Thermal transport properties including thermal conductivity, viscosity, and convective heat transfer coefficient of the nanofluids were further investigated.

S.-Z. Guo · J.-S. Jiang (✉)
Department of Physics, Center of Functional Nanomaterials and Devices, East China Normal University, 200241 Shanghai, China
e-mail: jsjiang@phy.ecnu.edu.cn

Y. Li · H.-Q. Xie (✉)
School of Urban Development and Environmental Engineering, Shanghai Second Polytechnic University, 201209 Shanghai, China
e-mail: hqxie@eed.sspu.cn

Experiment Details

Preparation of Nanofluids

Two-step method was used to prepare nanofluids. Commercial spherical-shaped γ-Fe_2O_3 nanoparticles with diameter of 20 nm were selected as additives, and the mixture of ethylene glycol and deionized water with volume ratio of 45:55 was selected as a base fluid. In a typical procedure, adequate surfactant (sodium oleate) was dissolved into the mixture at first, and then the nanoparticles were gradually added into the base mixture fluid with violent stirring. Afterward, the suspensions were stirred using disperse mill (7,200 r/min) for 40 min. Nanofluids with different volume fractions (φ, $\varphi = V_{nanoparticles}/V_{base\ fluids}$) of 0.005, 0.01, 0.015, and 0.02 were obtained by intensive ultrasonication for 45 min.

Measurement of Thermal Properties

The size of nanoparticles was observed by means of transmission electron microscope (TEM) (JEOL, *JEM-2100F*). The sample for TEM observation was prepared in a typical procedure. First, the nanoparticles were dispersed into the ethanol solution. Then, the mixture was ultrasonicated for 10 min to obtain stabilized suspension. Finally, the upper layer of the suspension was carefully selected to drop on a copper mesh.

The thermal conductivity of the nanofluids (k_{nf}) as a function of volume fraction of the nanofluids was measured using a transient short hot-wire method. Ethylene glycol was used to calibrate measurement apparatus. The thermal conductivity of ethylene glycol was measured threes times under a temperature at an interval of 5 min. The uncertainty of measurements is estimated to be within ±1.0%.

Viscosity of the base fluids or the nanofluids, η (mPa·s), was measured using a rotary viscometer (Brookfield, *DV-II + Pro*), which was calibrated using the standard fluid at first. The uncertainty of measurements is estimated to be within ±1.5%. The viscometer contains a sample chamber and a spindle. The fluid or nanofluid was put into the chamber, and the temperature of the sample, ranging from 10 to 60°C in 5°C increments in chamber, was controlled by water bath.

The convective heat transfer coefficient measurement setup shown in Fig. 1 is self-established, the convective heat transfer coefficient, h (W/m^2·K), was measured as a function of volume fraction of nanofluids in laminar flow region. The base fluids or the nanofluids was pumped to flow along the tube from reservoir containing fluids and back to the reservoir by a peristaltic pump (MasterFlex L/S, *MODEL 77202-50*). At the same time, the temperature of the heating bath and the cooling bath was controlled at 60°C and −15°C, respectively, to form a constant wall temperature boundary condition. Four T-Type thermocouples were used to measure the temperature at the outlet of the heating bath (T_w), the entrance of the cooling bath (T_1), 25 cm behind the entrance of the cooling bath (T_2), and inside the cooling bath, respectively. At last, the convective

Fig. 1 Schematic of experimental setup
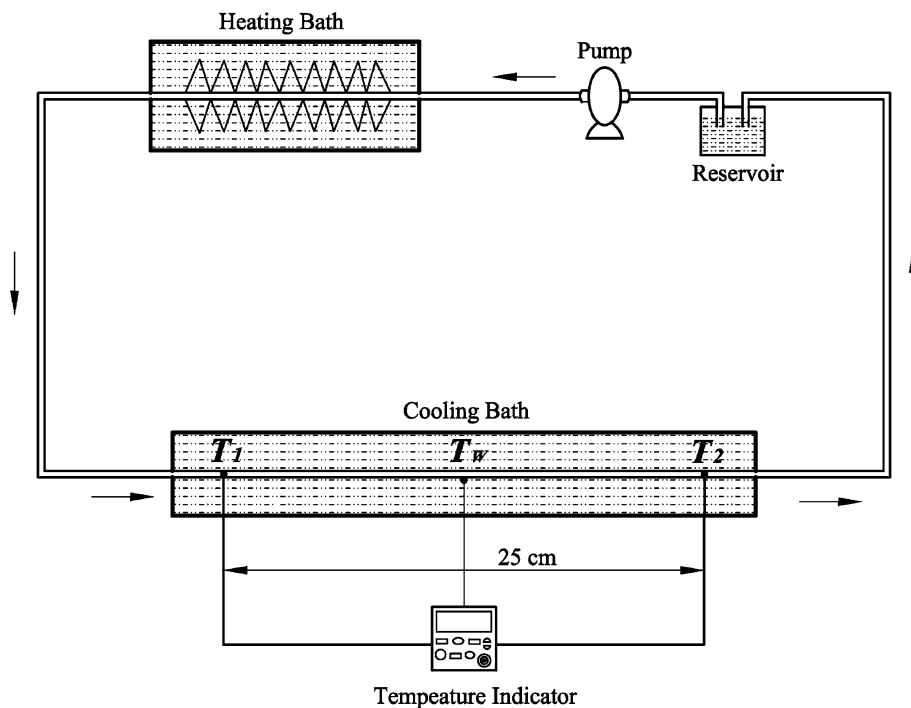
heat transfer coefficients can be easily determined according to the formula,

$$h = -\frac{\dot{m}C_p}{2\pi r \Delta L} \ln\frac{(T_w - T_2)}{(T_w - T_1)} \qquad (1)$$

where $\dot{m}, C_p$, r, and ΔL are the mass flow rates, the specific heat capacity, the radius of tube, and the length of tested region, respectively. Reynolds number, Re, was derived from
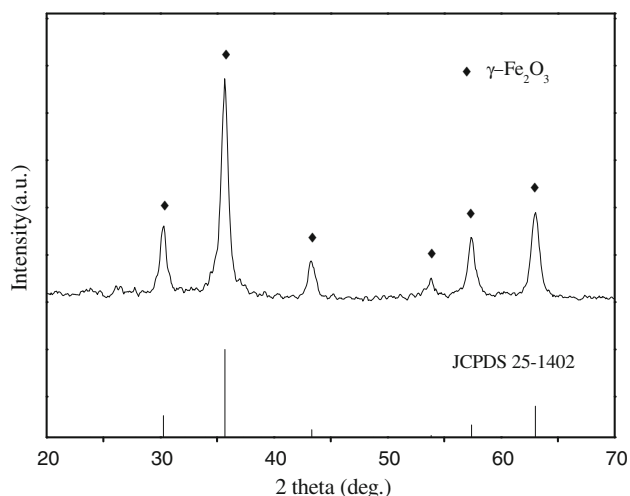
$$Re = \frac{\rho u D}{\eta} \qquad (2)$$

where ρ, u, D, and η are the density of the fluid, the flow rate of the fluid, the diameter of the tube, and the viscosity of the fluids, respectively.

Results and Discussion

The XRD pattern in Fig. 2 shows peaks at 30.272°, 35.684°, 43.34°, 53.852°, 57.4°, and 63.011°, which are corresponding to the diffraction peaks of γ-Fe$_2$O$_3$ (JCPDS 25-1402), indicating that nanoparticles are single phase with tetragonal structure. Figure 3 shows the TEM micrograph of γ-Fe$_2$O$_3$ nanoparticles. The average size of nanoparticles is estimated to be about 20 nm.
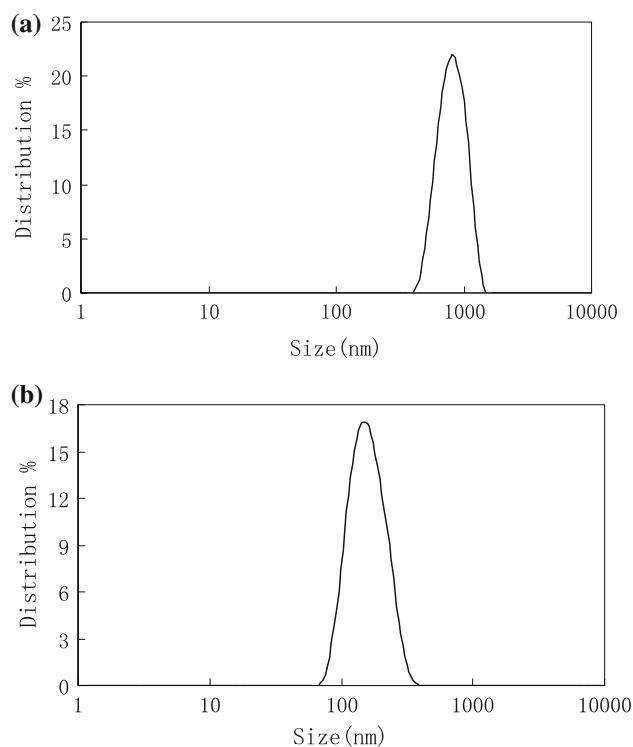
Figure 4 shows the particle size distributions in the magnetic nanofluids with and without surfactant, respectively. From Fig. 4, we can see that the average size is about 1,200 nm without surfactant (Fig. 4a) and about 150 nm with surfactant (Fig. 4b), respectively. When sodium oleate, a kind of organic salt, was dissolved into solution, the ionization of $C_{18}H_{33}O_2^-$ and Na^+ happens. One end of $C_{18}H_{33}O_2^-$ plunges into the solution, and another end was absorbed on the surface of nanoparticles.
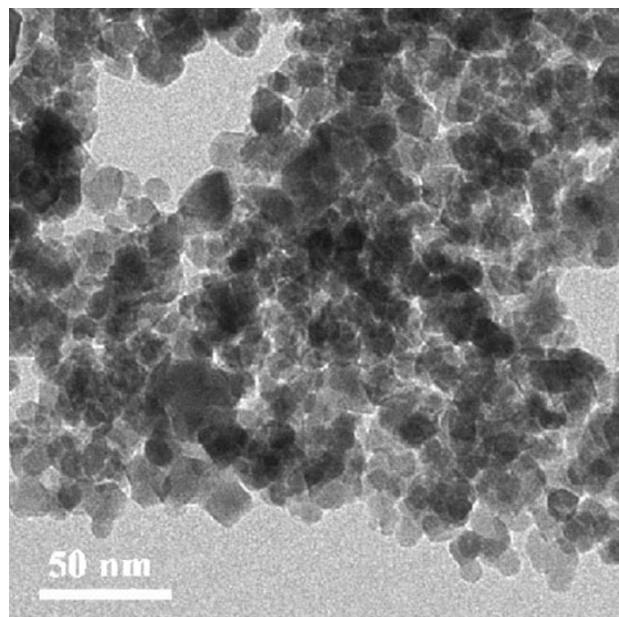

Fig. 3 TEM micrograph of the γ-Fe$_2$O$_3$ nanoparticles

Fig. 4 Particle size distribution in the nanofluids **a** without dispersant **b** with dispersant

With the addition of dispersant in the base fluids, the suspensions can keep stability for a long time, while sedimentation happened immediately in the suspensions without surfactant. Sodium oleate is effective for improving the stability of γ-Fe$_2$O$_3$ nanofluids.


Fig. 2 XRD pattern of γ-Fe$_2$O$_3$ nanoparticles
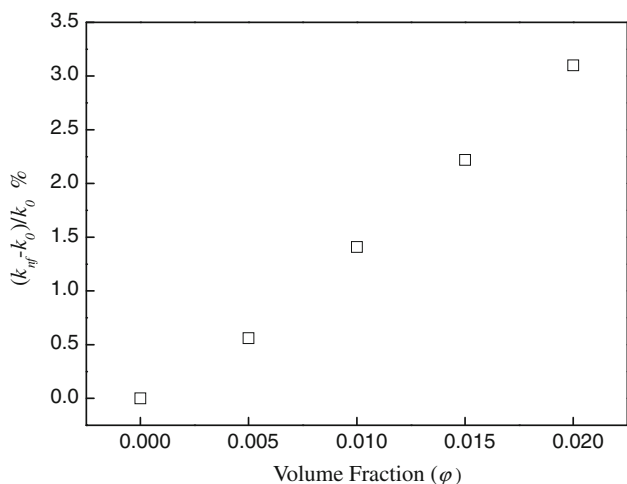
Fig. 5 Dependence of the enhanced ratios of the thermal conductivity on the volume fraction of γ-Fe$_2$O$_3$ nanoparticles

Fig. 6 Viscosity as a function of the volume fraction of γ-Fe$_2$O$_3$ nanoparticles and temperature

Figure 5 represents enhanced ratios $(k_{nf} - k_0)/k_0$ of the thermal conductivity of the nanofluids as a function of volume fraction (φ). It can be seen from Fig. 5 that the enhanced ratios of the thermal conductivity increase with the volume fraction of the nanoparticles. Unexpectedly, the conductivity of γ-Fe$_2$O$_3$ nanofluids was not so encouraging as previous investigation results for other kind of metal oxide nanofluids. For example, Zhu et al. [17] measured the thermal conductivity of Fe$_3$O$_4$/water nanofluids. They found that the ratios of the thermal conductivity enhanced by more than 15.0% even at the volume fraction of 0.005. Karthikeyan et al. [18] reported that the ratios of the thermal conductivity of CuO/water nanofluid enhancement were 31.6% with 1.0% CuO nanoparticles loading. The species of the dispersant may be the main reason to these differences. Sodium oleate that contains a long carbon-chain could improve the stability of γ-Fe$_2$O$_3$ nanoparticles suspending in the solution; however, it may also reduce the efficiency of heat transfer between the particles.

Viscosity is an important parameter in the pipeline flow. Figure 6 presents the results of the viscosity of the nano-fluids with different volume fractions as a function of temperature. It is shown that the viscosity of the nanofluids strongly depends on both temperature and volume. We observed that the viscosity of the nanofluids increases with the augment of the volume fraction but decreases with an increase in the temperature. Nguyen et al. [6] measured the viscosity of Al$_2$O$_3$/water nanofluids, which showed the same trend as well. Figure 7 depicts the rheological behaviors of the nanofluids with different particle loadings. The behaviors of the nanofluids from the Fig. 7 are close to the typical Newtonian fluids. Yu et al. [19] measured the viscosity of ZnO/EG nanofluids against shear rate. The results also showed that the viscosity of nanofluids
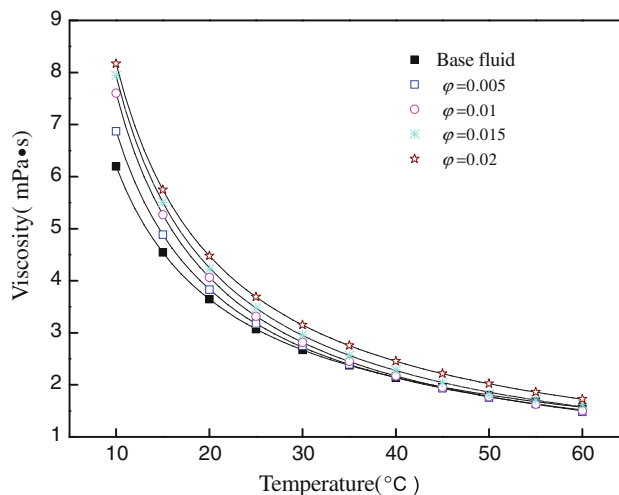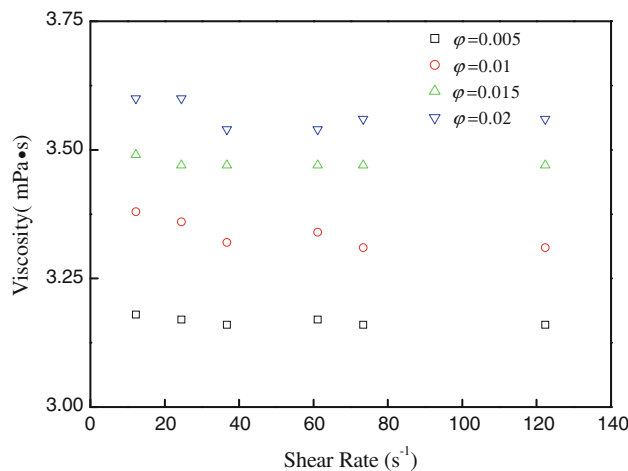

Fig. 7 Viscosity as a function of shear rate

increased with the increasing of particle concentrations and decreased with the augment of temperature. And they observed that the nanofluid demonstrated Newtonian behaviors and non-Newtonian behaviors at lower $(\varphi < 0.02)$ and higher $(\varphi > 0.03)$ volume fractions, respectively. Some theoretical predictions of viscosity (Einstein model [20], Brinkman model [21]) about the fluid were employed to compare with experiments of the nanofluids in Fig. 8. It is found that the experiment data of the nanofluids is much larger than the theoretical predictions values. The result may ascribe to the specific surface areas of the nanoparticles. The enhancement of viscosity may due to the very large surface area of the nanoparticles in the nanofluids [22]. Furthermore, the reason of the discrepancy may due to the nanoparticles size, which has an important effect on viscosity of nanofluids. When the diameter of the nanoparticles is less then 20 nm, the viscosity of nanofluids will increase rapidly as the diameters decrease [23].
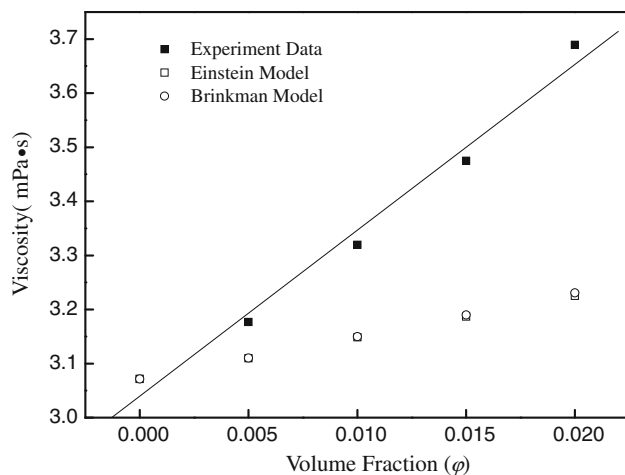
Fig. 8 Comparison of experimental data with theoretical predictions
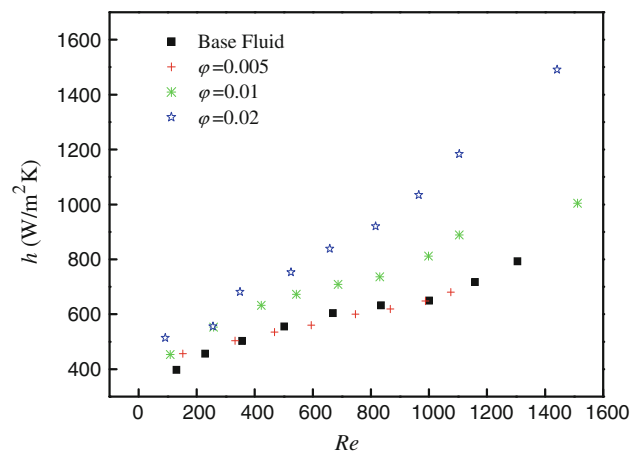
Fig. 9 Heat transfer coefficients versus Reynolds numbers for γ-Fe$_2$O$_3$ nanofluids

The convective heat transfer coefficient of the nanofluids with different volume fractions as a function of Reynolds number (Re) was shown in Fig. 9. It is seen that an augmentation of volume fraction or Reynolds number can make the heat transfer coefficient increase. It should be noted that though the conductivity of γ-Fe$_2$O$_3$ nanofluids was not encouraging in our experiment, the convective heat transfer coefficient increases with Reynolds number and volume fraction. The behaviors of convective heat transfer are similar to the base fluids at the volume fraction of 0.005, which may be due to the adhesion of nanoparticles on tube wall. Obviously, from the volume fraction of 0.01, the convective heat transfer coefficient enhanced quickly. For the nanofluid with a volume fraction of 0.02, the convective heat transfer coefficient can be enhanced by more than 60.0% at Reynolds number of 1,000. The viscosity value of the nanofluids in our experiment was nearly close to the base fluid especially at a higher temperature. The higher viscosity of nanofluids may suppress flow

turbulence [24]. Furthermore, the nanofluids with homogeneous and stable property may be also a critical factor to this result. Heris et al. [8] reported that the nanoparticles in a fluid changed the flow structure. Heat transfer enhancement of the nanofluids is not only related to the conductivity of nanofluids but also related to chaotic movements, dispersions, and so on.

Conclusions

We presented a technical route for preparing stable nanofluids composed of γ-Fe$_2$O$_3$ nanoparticles and the mixture of deionized water (DW) and ethylene glycol (EG) (DW-EG) as the base fluid. Sodium oleate was used as surfactant, and it was proved to be beneficial to the dispersion of the nanoparticles in the nanofluids. The viscosity of the γ-Fe$_2$O$_3$ nanofluids fits Newtonian behavior and strongly depends on the temperature and the volume fraction. Thermal conductivities of the nanofluids are higher than that of base fluid, and the enhanced values increase with the volume fraction of the nanoparticles. Though the enhanced ratios of thermal conductivity of the nanofluids are not so encouraging compared with other oxides nanofluids, the convective heat transfer coefficient of the nanofluids has substantial enhancement when compared to that of the base fluid. These results indicate that the enhanced thermal conductivity is not the only mechanism responsible for heat transfer enhancement and other factors such as stability of nanofluids, thermal properties, and viscosity of the nanofluids also should be considered.

References

1. L.F. Chen, H.Q. Xie, Y. Li, W. Yu, Thermochim. Acta **477**, 21 (2008)
2. T.K. Hong, H.S. Yang, C.J. Choi, J. Appl. Phys. **97**, 064311 (2005)
3. J. Garg, B. Poudel, M. Chiesa, J.B. Gordon, J.J. Ma, J.B. Wang, Z.F. Ren, Y.T. Kang, H. Ohtani, J. Nanda, G.H. McKinley, G. Chen, J. Appl. Phys. **103**, 074301 (2008)
4. H.Q. Xie, J.C. Wang, T.G. Xi, Y. Liu, F. Ai, Q.R. Wu, J. Appl. Phys. **91**(7), 4568 (2002)

5. P.K. Namburu, D.P. Kulkarni, D. Misra, D.K. Das, Exp. Therm. Fluid Sci. **32**, 397 (2007)
6. C.T. Nguyen, F. Desgranges, N. Galanis, G. Roy, T. Maréd, S. Boucher, H.A. Mintsa, Int. J. Therm. Sci. **47**, 103 (2008)
7. S.E.B. Maiga, C.T. Nguyen, N. Galanis, G. Roy, Superlattices Microstruct. **35**, 543 (2004)
8. S.Z. Heris, S.G. Etemad, M.N. Esfahany, Int. J. Heat Mass Transf. **33**, 529 (2006)
9. D.S. Wen, Y.L. Ding, Int. J. Heat Mass Transf. **47**, 5181 (2004)
10. Z. Bhimani, B. Wilson, Ind. Lubr. Tribol. **49**, 288 (1997)
11. A. Hatch, A.E. Kamholz, G. Holman, P. Yager, K.F. Böhringer, J. Microelectromech. Syst. **10**(2), 215 (2001)
12. J.S. Jiang, Z.F. Gan, Y. Yang, B. Du, M. Qian, P. Zhang, J. Nanopart. Res. **11**, 1321 (2009)
13. Z.F. Gan, J.S. Jiang, Y. Yang, B. Du, M. Qian, P. Zhang, J. Biomed. Mater. Res. **84A**, 10 (2008)
14. Y. Yang, J.S. Jiang, B. Du, Z.F. Gan, M. Qian, P. Zhang, J. Mater. Sci. Mater. Med. **20**(1), 301 (2009)
15. J. Philip, P.D. Shima, B. Raj, App. Phys. Lett. **92**, 043108 (2008)
16. D.P. Kulkarni, R.S. Vajjha, D.K. Das, D. Oliva, Appl. Therm. Eng. **28**, 1774 (2008)
17. H.T. Zhu, C.Y. Zhang, S.Q. Liu, Y.M. Tang, Y.S. Yin, App. Phys. Lett. **89**, 023123 (2006)
18. N.R. Karthikeyan, J. Philip, B. Raj, Mater. Chem. Phys. **109**, 50 (2008)
19. W. Yu, H.Q. Xie, L.F. Chen, Y. Li, Thermochim. Acta **491**, 92 (2009)
20. A. Einstein, *Investigations on the theory of the Brownian movement* (Dover Publications, New York, 1956)
21. H.C. Brinkman, J. Chem. Phys. **20**, 571 (1952)
22. H.Q. Xie, L.F. Chen, Q.R. Wu, High Temp.-High Pressures **37**, 127 (2008)
23. J.F. Zhao, Z.Y. Luo, M.J. Ni, K.F. Cen, Chin. Phys. Lett. **26**(6), 066202 (2009)
24. Q. Li, Y.M. Xuan, Sci. China Ser. E **45**(4), 408 (2002)